Journal of the Korean Electrochemical Society
Vol. 15, No. 2, 2012, 90-94
http://dx.doi.org/10.5229/JKES.2012.15.2.90

TiO_2@carbon Core-Shell Nanostructure Electrodes for Improved Electrochemical Properties in Alkaline Solution

Do-Young Kim, Young-Woo Lee, Sang-Beom Han, A-Ra Ko, Hyun-Su Kim, Si-Jin Kim, Sang-Eun Oh†, and Kyung-Won Park*

Department of Chemical Engineering, Soongsil University, Seoul 156-743, Korea
†Department of Biological Environment, Kangwon National University, Chuncheon, Gangwondo 200-701, South Korea

(Received March 31, 2012 : Accepted May 21, 2012)

Abstract : We report nanostructure electrodes with TiO_2 as a core and carbon as a shell (TiO_2@C) for oxygen reduction in alkaline solution. The structure of core-shell electrodes is characterized by transmission electron microscopy, Raman spectroscopy, X-ray diffraction method, and X-ray photoelectron microscopy. The electrochemical properties of the TiO_2@C electrodes are characterized using a potentiostat and compared with those of carbon supported Pt catalyst. In particular, the core-shell electrode with dominant pyridinic-N component exhibits an imporved electrocatalytic activity for oxygen reduction reaction in alkaline solution.

Keywords : Nanostructure materials, Core/shell, N-doping, Oxygen reduction reaction

1. Introduction

Oxygen reduction reaction (ORR) is one of the crucial characteristics in electrochemical energy conversion devices such as polymer electrolyte membrane fuel cells. The electrocatalytic ORR in alkaline fuel cells has attracted an intensive interest in alternative to Pt-based catalysts, although the ORRs in alkaline solutions are much faster than those in the acidic media.[1-6] Furthermore, the search for a low-cost, stable and more active electrocatalysts for the ORR in alkaline medium is thus of great importance.[7,8]

Nitrogen-doped carbon materials have exhibited much higher ORR activity than undoped carbon materials.[9-13] Nitrogen incorporation could chemically present active sites into the carbon for the electrocatalytic reactions.[14-16] The pyridinic nitrogen doped the carbon substrate's surface is shown to play important roles in the active sites for the ORR.[17-19] In particular, TiO_2 has been proposed as a good candidate for an electrode due to its chemical stability, cheapness, and nontoxicity.[20]

Herein, the nanostructure catalysts (TiO_2@C) consisting of TiO_2 as a core and carbon as a shell were prepared for oxygen reduction reaction in alkaline solution. The particle size, crystal structure, and chemical components of the catalysts were characterized using transmission electron microscopy (TEM), Raman spectroscopy, X-ray diffraction (XRD) method and X-ray photoelectron spectroscopy (XPS). The electrochemical properties of the catalysts were characterized using a potentiostat.

2. Experimental

2.1. Synthesis of catalysts

The nanostructure catalysts used TiO_2 (Degussa, P-25) as a starting material were prepared by means of heat treatment under CH_4 gas atmosphere. At first, the flow rate of N_2 gas was kept for 15 min to get rid of O_2 inside the tube. Under CH_4 flow rate of 100 mL min^{-1}, the furnace was heated from room temperature to 700°C and then maintained for 5 h. After the

*E-mail: kwpark@ssu.ac.kr

heat treatment for 5 h, the furnace was cooled down to room temperature under methane atmosphere. To prepare nitrogen-doped TiO_2@C catalysts, the FeTMPP (5,10,15,20-tetrakis(4-methoxyphenyl)-21H,23H-porphine iron(III) chloride, Aldrich) were dissolved in 99.7% acetic acid (2 ml, Aldrich) and acetone (90 ml, Aldrich) with continuous stirring for 1 h. After completely dissolving, the TiO_2@C powders were added slowly into the solutions to form a homogeneous blended solution by adsorbing the FeTMPP on the TiO_2@C. The solutions were completely evaporated and then dried at 50°C. The obtained powders were heated at 700°C for 5 h under N_2 flow rate of 50 mL min^{-1} and then cooled down to room temperature under N_2 atmosphere.

2.2. Structural analysis

TEM analysis of the catalysts was performed on a field emission transmission electron microscope (Tecnai G2 F30 system). TEM samples were prepared by placing drops of catalyst suspension dispersed in ethanol on a carbon-coated copper grid. Raman spectra were recorded on Mirco-Raman spectrometer (Jobin Yvon HR800 UV) using an Ar ion laser with $\lambda = 514.5$ nm. XRD analysis was carried out using Rigaku X-ray diffractometer with Cu K_α ($\lambda = 0.15418$ nm) source with a Ni filter. The source was operated at 40 kV and 100 mA. The 2θ angular scan from 20° to 60° was explored at a scan rate of 5° min^{-1}. The resolution in the scans was kept at 0.02°. XPS (Thermo Scientific, K-Alpha) analysis was carried out with the Al K_α X-ray source of 1486.8 eV at the chamber pressure below 1×10^{-8} Torr and 200 W beam power. All high resolution spectra were collected using a pass energy of 46.95 eV. The step size and time per step were chosen to be 0.025 eV and 100 ms, respectively. Both ends of the baseline were set sufficiently far so as not to distort the shape of spectra, including tails. Small variation of the range of the base line did not affect the relative amount of fitted species (less than 1%). The C 1 s electron binding energy was referenced at 284.6 eV and a nonlinear least-squares curve-fitting program was employed with a Gaussian-Lorentzian production function.

2.3. Electrochemical analysis.

Electrochemical properties of the catalysts were measured in a three-electrode cell at 25°C using a potentiostat (CH Instrument, CHI 700 C). The Pt wire and Hg/HgO (in saturated NaOH) were used as a counter and reference electrode, respectively. The rotating ring disk electrode as a

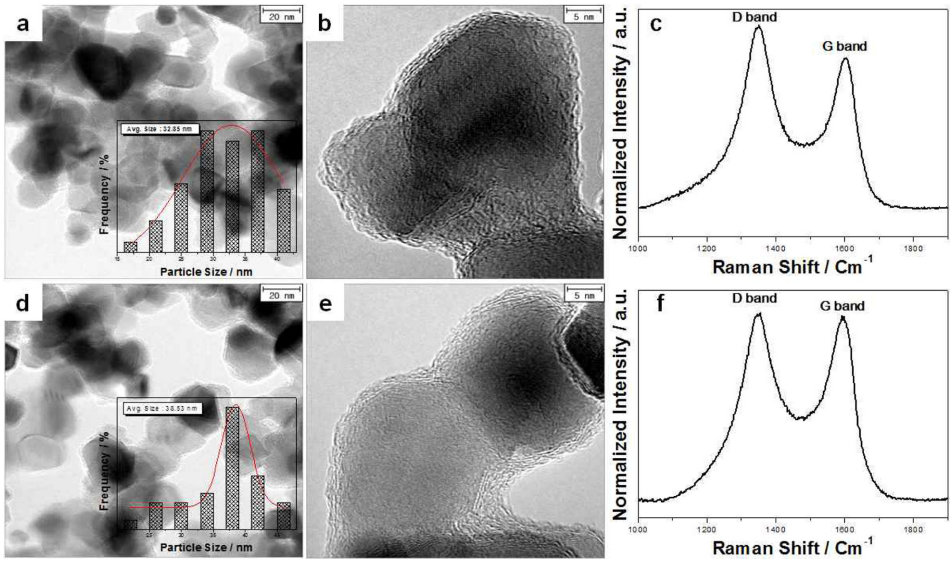

Fig. 1. TEM images of TiO_2@C (a,b) and TiO_2@C-N (d,e). The insets indicate particle size histograms of the catalysts. Raman spectra of TiO_2@C (c) and TiO_2@C-N (f).

working electrode was polished with 1, 0.3, and 0.05 μm Al_2O_3 paste and then washed in deionized water. The catalyst inks were prepared by ultrasonically dispersing catalyst powders (20 mg) in NMP (N-Methyl-2-pyrrolidone) solution (15 μL) containing 5 wt% PVDF (Polyvinylidene fluoride). The catalyst ink was dropped 1.57 μL onto a rotating ring disk electrode. After drying in 50°C oven, the total loading (~500 μg cm^{-2}) of all catalysts was identically deposited on the glassy carbon electrode. To compare electrochemical properties and ORR activity of the catalysts, characteristic curves were obtained between −0.6 and 0 V in 0.1 M NaOH. The current-potential curves for the ORR were obtained using cyclic and linear sweep voltammetry in O_2-saturated 0.1 M NaOH.

3. Results and discussion

Fig. 1 shows TEM images of the nanostructure catalysts for ORR. Compared to ~30 nm of commercial TiO_2 as a starting material, the average size of the TiO_2 heated at 700°C in CH_4 atmosphere is ~35 nm resulting from the increase of size due to heating process. Furthermore, it is observed that the undoped nanostructure catalyst (TiO_2@C) consists of core and shell structure (Fig. 1(a)). As shown in HR-TEM image of Fig. 1(b), the d-spacing of the core structure corresponds to that of TiO_2 (0.327 nm) whereas the d-spacing of the shell structure corresponds to that of graphitic layer (0.342 nm), which is similar to d-spacing of 0.335 nm of typical graphite. The measured thickness of the shell in the catalyst is ~2.0 nm. For N-doping in the TiO_2@C, FeTMPP was deposited on carbon layers and then pyrolyzed under N_2 atmosphere (referred as TiO_2@C-N). The TiO_2@C-N (Fig. 1(d),(e)) exhibits core-shell nanostructure similar to TiO_2@C. The measured thickness of the shell in the TiO_2@C-N is ~2.0 nm. As shown in HR-TEM images of Fig. 1(e), the core structures correspond to TiO_2 whereas the shell structures correspond to graphitic layer. The particle sizes of TiO_2@C and TiO_2@C-N are 32.85 and 38.53 nm, respectively (the insets of Fig. 1). The Raman spectra of the catalysts consist of two main peaks: a G-band at ~1590 cm^{-1} resulting from the in-plane stretching vibration mode E_{2g} of single crystal graphite and a D-band at ~1345 cm^{-1} representing the disorder-induced characteristics (Fig. 1(c),(f)). The TiO_2@C-N exhibits relatively low I_D/I_G ratio, suggesting an improved crystallinity of carbon despite the nitrogen doping as compared to the TiO_2@C.

Typically, the commercial TiO_2 (Degussa, P-25) consists of dominant anatase and rutile phase. In contrast, the heated TiO_2 samples display mixed phases of anatase and dominant rutile, which means phase transformation of anatase into rutile phase (Fig. 2). It is observed that the anatase phase is transformed into the rutile phase at both heating temperatures. In general, it is known that the phase transformation from metastable anatase to stable rutile occurs at around 600°C . As shown in Fig. 3, the XPS peak of the catalyst contain three main portions of nitrogen to curve

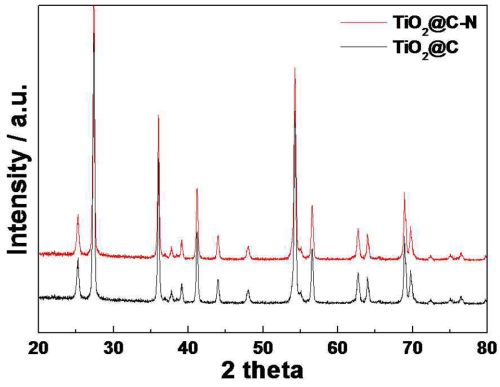

Fig. 2 XRD patterns of TiO2@C and TiO2@C-N.

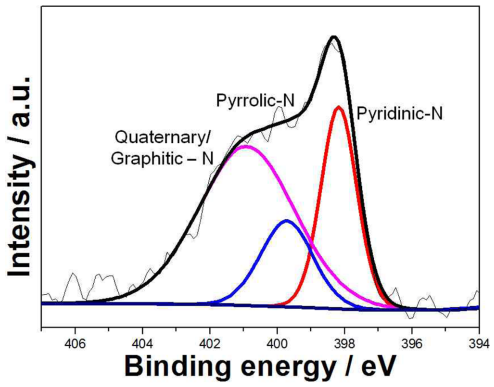

Fig. 3. XPS N1s spectrum of TiO_2@C-N.

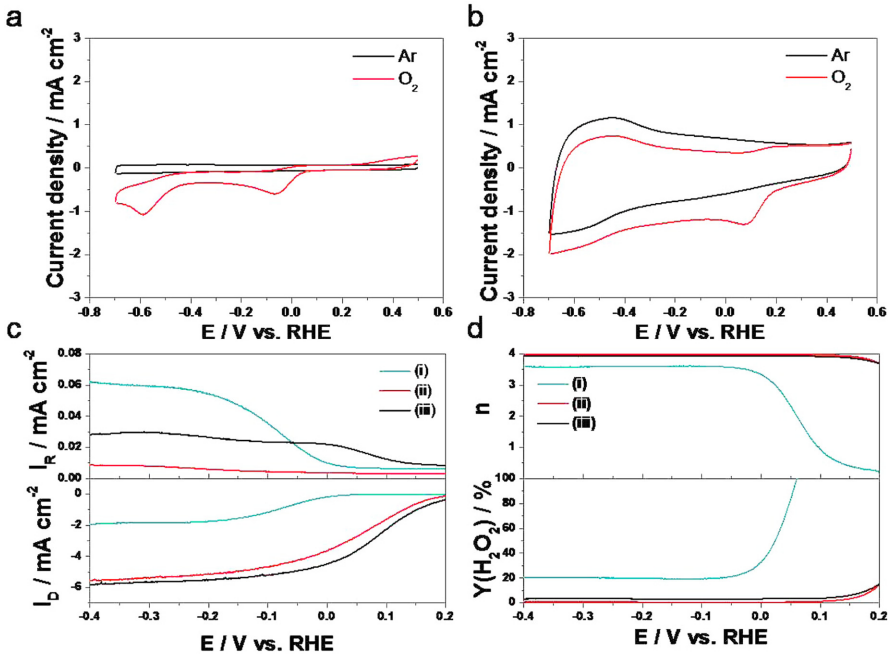

Fig. 4. CVs of TiO_2@C (a) and TiO_2@C-N (b) in 0.1 M NaOH with a scan rate of 50 mV s^{-1} at 25 °C. Polarization curves (c,d) of the TiO_2@C (i), TiO_2@C-N (ii), and Pt/C (iii) in O_2-saturated 0.1 M NaOH solution with a scan rate of 10 mV s^{1} and rotating speed of 1600 rpm at 25°C. The potential of the ring electrode was set to 0.15 V.

fit in the N 1s spectrum. For the TiO_2@C-N, the pyridinic-N and pyrrolic-N are assigned to the components at 398.1 and 400.3 eV, respectively, and the quaternary/graphitic-N is presented at 400.9 eV.

The ORR characteristics of the TiO_2@C and TiO_2@C-N in alkaline solution were evaluated using cyclic voltammetry (Fig. 4(a),(b)). The TiO_2@C-N exhibits higher onset potential and higher current density than those of the TiO_2@C indicating such an excellent ORR activity. Furthermore, to characterize ORR performance and mechanism of these catalysts, rotating ring disk electrode analysis was carried out. The onset potential of the TiO_2@C-N toward ORR in the polarization curves is significantly shifted to positive direction still lower than that of Pt/C, as compared with the TiO_2@C (Fig. 4(c)). The disk current density (I_D) of the TiO_2@C-N is much larger than that of the TiO_2@C, whereas the ring current density (I_R) of the TiO_2@C-N is comparably smaller than that of TiO_2@C. The plots of the number of exchanged electrons (*n*) and the generation yield (%H_2O_2) of hydrogen peroxide during ORR versus electrode potentials are as shown in Fig. 4(d). The *n* exchanged by the TiO_2@C-N toward ORR is determined to be approximately 4.0 as compared to 3.3~3.5 of the TiO_2@C indicating that O_2 reduction reaction catalyzed on the TiO_2@C-N is an apparent near four electron transfer process comparable to that of the Pt/C below −0.1 V. For the Pt/C, no signficant H_2O_2 yield is detected in the range of less than 5% (Fig. 4(d)). The %H_2O_2 generated by the TiO_2@C-N is much lower (~3%) than that of the TiO_2@C (~20%). It is likely that the improved ORR of the TiO_2@C-N as a core-shell nanostructure catalyst may result from nitrogen doping and pyridinic-N.

4. Conclusion

We have prepared the nanostructure catalysts with TiO_2 as a core and carbon as a shell for ORR in alkaline solution. The TiO_2@C-N catalyst exhibits nitrogen-doped carbon layers on TiO_2

nanoparticles. The excellent ORR activity of the TiO_2@C-N may be mainly due to N-doping effect of pyridinic-N component.

Acknowledgments

This work was supported by the Human Resources Development of the Korea Insitute of Energy Technology Evaluation and Planning(KETEP) grant funded by the Ministry of Knowledge Economy, Republic of Korea. (No. 20104010100610)

References

1. H. Li, H. Liu, Z. Jong, W. Qu, D. Geng, X. Sun and H. Wang, 'Nitrogen-doped carbon nanotubes with high activity for oxygen reduction in alkaline media', *Int. J. Hydrog. Energy*, **36**, 2258 (2011).
2. Q. Yue, K. Zhang, X. Chen, L. Wang, J. Zhao, J. Liu and J. Jia, 'Generation of OH radicals in oxygen reduction reaction at Pt–Co nanoparticles supported on graphene in alkaline solutions', *Chem. Commun*., **46**, 3369 (2010).
3. K.P. Gong, F. Du, Z.H. Xia, M. Durstock and L.M. Dai, 'Nitrogen-doped carbon nanotube arrays with high electrocatalytic activity for oxygen reduction', *Science*, **323**, 760 (2009).
4. Y. Tang, B.L. Allen, D.R. Kauffman and A. Star, 'Electrocatalytic activity of nitrogen-doped carbon nanotube cups', *J. Am. Chem. Soc*., **131**, 13200 (2009).
5. T. Iwazaki, R. Obinata, W. Sugimoto and Y. Takasu, 'High oxygen-reduction activity of silk-derived activated carbon', *Electrochem. Commun*., **11**, 376 (2009).
6. R.A. Sidik, A.B. Anderson, N.P. Subramanian, S.P. Kumaraguru and B.N. Popov, 'O_2 reduction on graphite and nitrogen-doped graphite: experiment and theory', *J. Phys. Chem. B*, **110**, 1787 (2006).
7. T. C. Nagaiah, S. Kundu, M. Bron, M. Muhler and W. Schuhmann, 'Nitrogen-doped carbon nanotubes as a cathode catalyst for the oxygen reduction reaction in alkaline medium', *Electrochem. Commun*., **12**, 338 (2010).
8. S. H. Joo, S. J. Choi, I. Oh, J. Kwak, Z. Liu, O. Terasaki and R. Ryoo, 'Ordered nanoporous arrays of carbon supporting high dispersions of platinum nanoparticles', *Nature*, **412**, 169 (2001).
9. S. Shanmugam and T. Osaka, 'Efficient electrocatalytic oxygen reduction over metal free-nitrogen doped carbon nanocapsules', *Chem. Commun*., **47**, 4463 (2011).
10. Z. Chen, D. Higgins and Z. Chen, 'Electrocatalytic activity of nitrogen doped carbon nanotubes with different morphologies for oxygen reduction reaction', *Electrochim. Acta*, **55**, 4799 (2010).
11. M. Lefèvre and J. P. Dodelet, 'Fe-based catalysts for the reduction of oxygen in polymer electrolyte membrane fuel cell conditions: determination of the amount of peroxide released during electroreduction and its influence on the stability of the catalysts', *Electrochim. Acta*, **48**, 2749 (2003).
12. G. Lalande, R. Côté, D. Guay, J. P. Dodelet, L. T. Weng and P. Bertrand, 'Is nitrogen important in the formulation of Fe-based catalysts for oxygen reduction in solid polymer fuel cells?', *Electrochim. Acta*, **42**, 1379 (1997).
13. V. V. Strelko, V. S. Kuts and P. A. Thrower, 'On the mechanism of possible influence of heteroatoms of nitrogen, boron and phosphorus in a carbon matrix on the catalytic activity of carbons in electron transfer reactions', *Carbon*, **38**, 1499 (2000).
14. R. Wang, J. Jia, H. Li, X. Li, H. Wang, Y. Chang, J. Kang and Z. Lei, 'Nitrogen-doped carbon coated palygorskite as an efficient electrocatalyst support for oxygen reduction reaction', *Electrochim. Acta*, **56**, 4526 (2011).
15. S. V. Dommele, K. P. Jong and J. H. Bitter, 'Nitrogen-containing carbon nanotubes as solid base catalysts', *Chem. Commun*., **48**, 4859 (2006).
16. A. Zamudio, A. L. Elýas, J. A. Rodríguez-Manzo, F. López-Urías, G. Rodríguez-Gattorno, F. Lupo, M. Rühle, D. J. Smith, H. Terrones, D. Díaz and M. Terrones, *Small*, **3,** 346 (2006).
17. X. Li , B. N. Popov, T. Kawahara and H. Yanagi, 'Non-precious metal catalysts synthesized from precursors of carbon, nitrogen, and transition metal for oxygen reduction in alkaline fuel cells', *J. Power Sources*, **196**, 1717 (2011).
18. P. H. Matter, L. Zhang and U. S. Ozkan, 'The role of nanostructure in nitrogen-containing carbon catalysts for the oxygen reduction reaction', *J. Catal*., **239**, 83 (2006).
19. K. A. Kurak and A. B. Anderson, 'Nitrogen-treated graphite and oxygen electroreduction on pyridinic edge sites', *J. Phys. Chem. C*, **113**, 6730 (2009).
20. L. Xiong, and A. Manthiram, 'Synthesis and characterization of methanol tolerant Pt/TiOx/C nanocomposites for oxygen reduction in direct methanol fuel Cells', *Electrochim. Acta*, **49**, 4163 (2004).